

Nearly frozen Coulomb liquids

Y. Pramudya, H. Terletska, S. Pankov, E. Manousakis, and V. Dobrosavljević
*Department of Physics and National High Magnetic Field Laboratory,
 Florida State University, Tallahassee, Florida 32310*

We show that very long-range repulsive interactions of a generalized Coulomb-like form $V(R) \sim R^{-\alpha}$, with $\alpha < d$ (d -dimensionality), typically introduce very strong frustration, resulting in extreme fragility of the charge-ordered state. An "almost frozen" liquid then survives in a broad dynamical range above the (very low) melting temperature T_c which is proportional to α . This "pseudogap" phase is characterized by unusual insulating-like, but very weakly temperature dependent transport, similar to experimental findings in certain low carrier density systems.

PACS numbers: 71.30.+h, 71.27.+a

I. INTRODUCTION

In designing novel materials, lightly doping a parent insulator is typically the method of choice. An especially intriguing situation is found in ultra-clean samples at finite doping, where neither the Anderson¹ (disorder-driven) nor the Mott² (magnetism-driven) route for localization can straightforwardly succeed in trapping the electrons. The tendency for charge ordering (CO) then emerges as the dominant mechanism that limits the electronic mobility. As first noted in early works by Wigner³ and Mott², this is precisely where the incipient breakdown of screening reveals the long-range nature of the Coulomb interactions. The corresponding CO states proved to be of extraordinary fragility, restricting the insulating behavior to extremely low densities and/or temperatures⁴. A broad range of parameters then emerges where puzzling "bad insulator" transport characterizes such *nearly-frozen Coulomb liquids*.

Unusual "bad-insulator" transport behavior has been observed in many systems. Examples range from high mobility two-dimensional electron systems in semiconductors,⁵ to lightly-doped cuprates,^{6,7} manganites,⁸ and even to the behavior of lodestone (magnetite) above the Verwey transition.⁹ In all these cases, a broad range of temperatures has been observed, where the resistivity rises at low temperatures, but it does so with surprisingly weak temperature dependence. In contrast to conventional insulators, where the familiar activated transport reflects a gap for charge excitations, the "bad insulator" behavior has been interpreted⁹ as a *precursor* to charge ordering, leading to very gradual opening of a soft pseudogap in the excitation spectrum.

The physical picture of a *nearly-frozen Coulomb liquid* has been proposed on a heuristic level by several authors,⁹⁻¹¹ providing a plausible and appealing interpretation of many experiments. The interplay of spins and charge degrees of freedom in pseudogap formation is still a controversial and unresolved problem. Therefore, to focus on the corresponding role of charge fluctuations, we deliberately ignore any spin effects, and consider a class of models of spinless electrons interacting through long-range interactions.

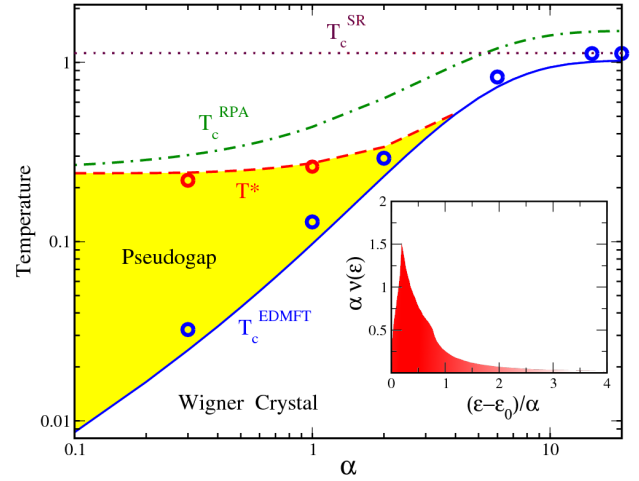


Figure 1: (Color online) Phase diagram of the half-filled classical $d = 3$ lattice model with interactions $V(R) = R^{-\alpha}$. The charge ordering temperature $T_c(\alpha) \sim \alpha$, as obtained from EDMFT theory (full line) and Monte-Carlo simulations (open symbols). The pseudogap temperature T^* (dashed line) remains finite as $\alpha \rightarrow 0$; a broad pseudogap phase emerges at $\alpha \leq d$. We also show $T_c^{SR} \approx 1$ for the same model with short-range interactions (dotted line), and T_c^{RPA} (dot-dashed line) from the classical limit of RPA. The inset shows the corresponding plasmon mode spectral density, which assumes a scaling form for $\alpha \ll 1$. The fluctuations of these very soft "sheer plasmons" lead to the dramatic decrease of T_c .

We present the simplest consistent theory of this strongly coupled liquid state. We demonstrate that the existence of such an intermediate liquid regime, which emerges at $k_B T_c < k_B T \ll E_c$ (see below), is a very general phenomenon reflecting strong frustration produced by long-range interactions. It holds for any interaction of the form $V(R) \sim R^{-\alpha}$, both in continuum and lattice models at any dimension $d \geq 2$, with $\alpha \ll d$. Ours is a microscopic theory that substantiates this physical picture,^{9,11} based on quantitative and controlled model calculations. We present a physically transparent analytical description using extended dynamical mean-field theory (EDMFT) to accurately describe the collective charge fluctuations, and benchmark our result using Monte-

Carlo MC simulations.

II. OUR MODEL AND THE EDMFT APPROACH

It has long been appreciated^{4,12,13} that in Coulomb systems, the CO temperature scale T_c is generally very small as compared to the Coulomb energy $E_c = e^2/a$ (a being typical inter-particle spacing), which we use as our energy unit. For example, for classical particles on a half-filled hypercubic lattice $T_c \approx 0.1$,¹² while in the continuum and classical Wigner crystal $T_c \approx 0.01$ ⁴; similar results are obtained both in $d = 2$ and in $d = 3$. Such large values of the “Ramirez index”¹⁴ $f = E_c/T_c$ suggest that geometric frustration plays a significant role, reflecting the long-range nature of the Coulomb force.

To clarify this behavior, we control the amount of frustration by introducing generalized Coulomb interactions of the form $V(R)/E_c = (R/a)^{-\alpha}$. We consider a lattice model of spinless electrons given by the Hamiltonian

$$H = - \sum_{ij} t_{ij} c_i^\dagger c_j + \frac{1}{2} \sum_{ij} V(R_{ij}) (n_i - \langle n \rangle) (n_j - \langle n \rangle). \quad (1)$$

Here c_i^\dagger and c_i are the electron creation and annihilation operators, t_{ij} are the hopping matrix elements, $n_i = c_i^\dagger c_i$, and R_{ij} is the distance between lattice sites i and j expressed in the units of the lattice spacing. The origin of frustration is then easily understood by noting that in the classical limit our lattice gas model ($n_i = 0, 1$) maps onto an Ising antiferromagnet ($S_i = \pm 1$) with long-range interactions. Here, the maximum level of frustration is achieved for infinite range interactions ($\alpha \rightarrow 0$), and any finite temperature ordering is completely suppressed.

A controlled theoretical approach to our problem is available for very long-range interactions ($\alpha \ll 1$), which effectively corresponds to a very large coordination number. In this limit the spatial correlations assume a simplified form

$$G_k(i\omega_n) = \langle c_k^\dagger c_{-k} \rangle = \frac{1}{i\omega_n - \epsilon_k - \Sigma(i\omega_n)},$$

$$\Pi_k(i\Omega_n) = \langle n_k n_{-k} \rangle = \frac{\tilde{\Pi}(i\Omega_n)}{\tilde{\Pi}(i\Omega_n) + V_k}, \quad (2)$$

where the momentum dependence of the (fermionic) self-energy $\Sigma(i\omega_n)$ and the irreducible polarization operator $\tilde{\Pi}(i\Omega_n)$ can be ignored²⁶. A conserving approximation that formally sums all the corresponding Feynman diagrams is given by the so-called EDMFT formulation,^{15–17} where the relevant (local) quantities are computed from an auxiliary local effective action

$$S_{eff} = - \int d\tau d\tau' c^\dagger(\tau) \mathcal{G}_0^{-1}(\tau - \tau') c(\tau') + \frac{1}{2} \int d\tau d\tau' \delta n(\tau) \Pi_0^{-1}(\tau - \tau') \delta n(\tau'), \quad (3)$$

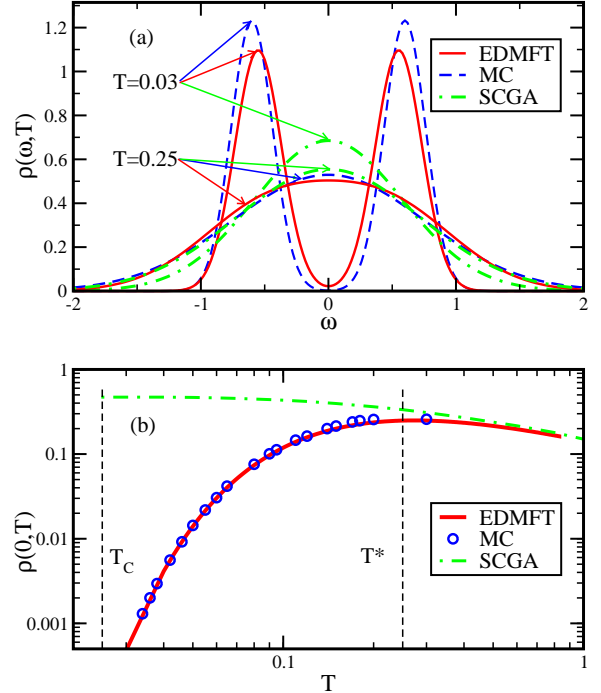


Figure 2: (Color online) (a) Density of states $\rho(\omega, T)$ obtained with three different methods: EDMFT (full line), MC (dashed line) and SCGA (dot-dashed line). Results are shown for the $d = 3$ half-filled cubic lattice with $t = 0$, $a = 0.3$, and two temperatures: $T = 0.03 \approx T_c$ and $T = 0.25 \approx T^*$. $\rho(\omega, T)$ obtained from EDMFT (full line) agree well with MC results (dashed line), while SCGA (dot-dashed line) does not account for the pseudogap formation. (b) Both EDMFT (full line) and MC results (open symbols) $\rho(\omega = 0, T)$ show pseudogap opening (dramatic DOS decrease) at $T < T^*$ in contrast to SCGA results (dot-dashed line).

where $\mathcal{G}_0^{-1}(i\omega) = i\omega - \Delta(i\omega)$ and $\delta n(\tau) = n(\tau) - \langle n \rangle$. The dynamical effective-medium (EM) functions Δ and Π_0^{-1} represent the respective fermionic and bosonic baths coupled to the given lattice site. For a given bath, the (local) Dyson’s equations stipulate that $\Sigma = \mathcal{G}_0^{-1} - G_{loc}^{-1}$ and $\tilde{\Pi}^{-1} = \Pi_{loc}^{-1} - \Pi_o^{-1}$, where G_{loc} and Π_{loc} are calculated directly from S_{eff} . The self-consistency loop is then closed by relating the local and the EM correlators, viz, $G_{loc} = \sum_k G_k(\Sigma)$ and $\Pi_{loc} = \sum_k \Pi_k(\tilde{\Pi})$.

III. CLASSICAL LIMIT

The most stringent test for the accuracy of EDMFT is provided by examining the classical limit ($t = 0$), where pseudogap formation is most pronounced. Here, the EDMFT equations can be solved in closed form,¹⁷ since the “memory kernel” $\Pi_0^{-1}(\tau - \tau')$ becomes a time-independent constant, $\Pi_0^{-1} = D/\beta^2$, and the corresponding mode-coupling term in Eq. (3) can be decoupled by a static Hubbard-Stratonovich transformation. The density correlator then assumes the form

$\Pi_k = (4 + D + \beta V_k)^{-1}$, and the self-consistency condition reduces to

$$\frac{1}{4} = \int d\varepsilon \nu(\varepsilon) (4 + D + \beta\varepsilon)^{-1}, \quad (4)$$

where we introduced the (classical) plasmon-mode spectral density $\nu(\varepsilon) = \sum_k \delta(\varepsilon - V_k)$. The CO critical temperature $T_c(\alpha)$ is identified by the vanishing of Π_k^{-1} at the corresponding ordering wave vector $k = Q$. The mechanism for T_c depression is then easily understood by noting that for $\alpha \ll 1$ the spectral density $\nu(\varepsilon)$ assumes the scaling form $\nu(\varepsilon) = \alpha^{-1} \tilde{\nu}((\varepsilon - \varepsilon_0)/\alpha)$, where $\varepsilon_0 \approx -1$; the explicit form of the scaling function $\tilde{\nu}(\varepsilon - \varepsilon_0)$ corresponding to the half-filled cubic lattice is shown in the inset of Figure 1. It features a sharp low-energy spectral peak of the usual dispersive form $\nu(\varepsilon) \sim \varepsilon^{(d-2)/2}$ only at $(\varepsilon - \varepsilon_0) < \varepsilon^*(\alpha)$, i.e below a characteristic energy scale $\varepsilon^*(\alpha) \sim \alpha$ and a long high-energy tail of the form $\nu(\varepsilon) \sim \varepsilon^{-2}$. Physically, these low energy excitations correspond to “sheer” plasmon modes with wave vector $k \approx Q$; the scale $\varepsilon^*(\alpha) \sim \alpha$ thus plays a role of an effective Debye temperature. Its smallness sets the scale for the ordering temperature $T_c(\alpha) = \alpha \int d\varepsilon \tilde{\nu}(\varepsilon)/\varepsilon \sim \varepsilon^*(\alpha)$, in agreement with an estimate based on a Lindemann criterion applied to the sheer mode²⁷.

In the classical limit, the single particle density of states (DOS) $\rho(\omega, T) \equiv -\text{Im}G(\omega + i0^+)/\pi$ assumes a simple bimodal form:

$$\rho(\omega, T) = \frac{\beta}{\sqrt{8\pi D}} \left\{ \exp \left[-\frac{\beta^2}{2D} \left(\omega + \frac{D}{2\beta} \right)^2 \right] + \exp \left[-\frac{\beta^2}{2D} \left(\omega - \frac{D}{2\beta} \right)^2 \right] \right\}, \quad (5)$$

with the self-consistently determined parameter $D(T)$ setting the scale of the Coulomb pseudogap (“plasma dip”) $E_{\text{gap}} = D/\beta$, which starts to open at the crossover temperature $T^* = D/4\beta$. We stress that, in contrast to the ordering temperature $T_c \sim \alpha$, both E_{gap} and T^* remain finite for $\alpha \ll 1$, since $D(T) \approx \beta$ in this limit. This leads to the emergence of a broad pseudogap regime for $\alpha \lesssim d$, independent of the precise form or the filling of the lattice. Remarkably, since $D(T)$ remains finite as $\alpha \rightarrow 0$, both the density of states $\rho(\omega, T)$ and the conductivity $\sigma(T)$ (see below) display only very weak α -dependence, in contrast to $T_c(\alpha) \sim \alpha$.

We benchmark these analytical predictions against MC simulations which used careful finite-size scaling analysis and (generalized) Ewald summation techniques to account for long-range interactions (the detail is in the appendix). It was found that EDMFT captures all qualitative and even quantitative features of the pseudogap regime for several different values of the exponent α , both in dimensions $d = 2$ and in $d = 3$. The detailed comparison of EDMFT and MC results will be presented elsewhere; here we illustrate these findings for a $d = 3$ half-

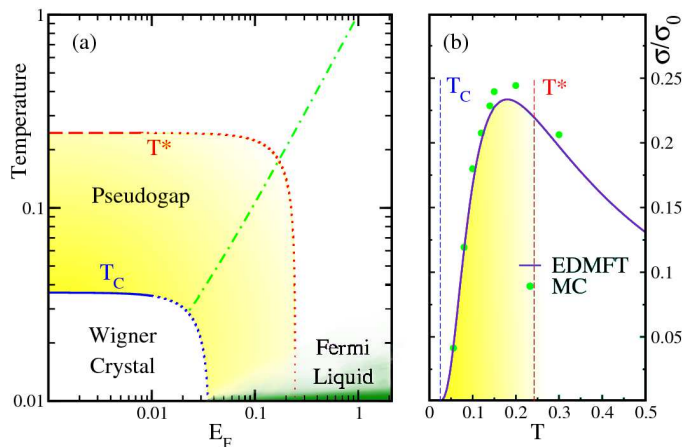


Figure 3: (Color online) (a) EDMFT phase diagram for a half-filled cubic lattice with $\alpha = 0.3$ as a function of temperature T and the electron’s Fermi energy $E_F \sim t$. Our semiclassical solution is valid above the CO freezing temperature $T_c(E_F)$ (full line), and the Fermi liquid crossover temperature $T_{\text{cros}}(E_F)$ (dot-dashed line). At intermediate temperatures $T_c < T < T^*$ we find well developed pseudogap behavior, where transport assumes insulating-like but very weak temperature dependence [as shown in (b)]; in the CO phase ($T < T_c$) transport assumes the conventional activated form (not shown). (b) Temperature dependence of the conductivity in the semiclassical regime ($E_F \ll 1$), where only the prefactor $\sigma_0 = \frac{\pi}{3} \frac{e^2 t^2}{\hbar a}$ displays significant t -dependence; EDMFT results (full line) again show remarkable agreement with results obtained by calculating $\rho(\varepsilon, \omega)$ in the classical limit using MC simulations (symbols).

filled cubic lattice. Figure 1 shows how EDMFT accurately captures the α -dependence of T_c , which is found to decrease in a roughly linear fashion as $\alpha \rightarrow 0$, while the $T^* \approx 0.25$ remains finite, producing a large separation of energy scales and a well-developed pseudogap regime. Note that the familiar Coulomb interaction ($\alpha = 1$) lies well within the small- α regime. This observation makes it clear why our EDMFT theory remains very accurate (as noted in previous work¹⁷) not only for $\alpha \ll 1$, but also for the physically relevant Coulomb case $\alpha = 1$.

IV. GAUSSIAN THEORIES DO NOT CAPTURE PSEUDOGAP FORMATION

The excellent comparison between EDMFT and MC results for the DOS is shown for $\alpha = 0.3$ in Figure 2(a). In contrast, the conventional approaches¹⁸, which typically assume Gaussian statistics for the collective charge fluctuations, fail to capture the pseudogap opening at $T > T_c$. For example, the familiar self-consistent Gaussian approximation (“spherical model”), while predicting the exact same T_c as EDMFT, produces Gaussian-shaped DOS at any $T > T_c$, in contrast with MC findings; these shortcomings are especially dramatic for $\alpha \ll d$ (see Figure 2). The popular “random-phase approxima-

tion" (RPA),¹⁹ which amounts to a non-self-consistent Gaussian approximation (SCGA), proves even less reliable in this regime. It grossly overestimates the freezing temperature T_c , which is found [dashed line in Figure 2 (b)] to remain finite even as $\alpha \rightarrow 0$, completely missing the pseudogap regime (shaded area in Figure 1). Physically, the RPA (Stoner-like) freezing criterion reduces to the simplistic Hartree (static mean-field) approximation, which ignores the dramatic fluctuation effects of the soft collective (sheer plasmon) modes.

V. BAD-INSULATOR TRANSPORT IN THE SEMICLASSICAL REGIME

We expect the “bad insulator” transport to be best pronounced in the semiclassical regime $t \ll 1$, where the Coulomb energy represents the largest energy scale in the problem. Here, the pseudogap phase is reached by thermally melting the CO state at $T > T_c(t)$. While our EDMFT equations are difficult to solve in general, in this incoherent regime it is well justified to utilize an adiabatic (“static”) approximation,¹⁸ which ignores the time dependence of the collective mode. The EDMFT equations can then be solved in a manner similar to that in the strict classical limit (see above), and we find

$$\begin{aligned} G(i\omega) &= \int d\phi G_\phi(i\omega) P(\phi), \\ \Pi(i\Omega) &= T \sum_{i\omega} \int d\phi G_\phi(i\omega + i\Omega) G_\phi(i\omega) P(\phi), \\ P(\phi) &= \frac{1}{Z} \exp \left(-\frac{D}{2} \phi(\phi + 1) - \sum_{\omega} \ln(G_\phi(i\omega)) \right), \\ G_\phi^{-1}(i\omega) &= G_0^{-1}(i\omega) + \phi T D. \end{aligned} \quad (6)$$

Physically, the electrons travel in the presence of a static, but spatially fluctuating random field representing the collective mode. Its probability distribution $P(\phi)$ assumes a strongly non-Gaussian character, reflecting the charge discreteness captured by EDMFT, but ignored by conventional Gaussian theories such as RPA.

The semiclassical approximation remains valid¹⁸ as long as the time-dependence of the density correlator $\Pi(\tau)$ can be ignored, corresponding to

$$|(\Pi(0) - \Pi(\beta/2))/\Pi(0)| \ll 1. \quad (7)$$

This criterion provides an estimate for the crossover temperature T_{cros} , below which we expect (at large t) a gradual crossover towards Fermi liquid behavior. The resulting phase diagram is shown on Figure 3 (a).

To calculate transport, we use the Kubo formula for the resistivity, which within the EDMFT theory assumes the form²⁰:

$$\sigma = \frac{\pi}{3} \frac{e^2 t^2}{\hbar a} \int_{-\infty}^{+\infty} d\varepsilon \int_{-\infty}^{+\infty} d\omega \rho_o(\varepsilon) \frac{A^2(\varepsilon, \omega)}{4T \cosh^2 \frac{\omega}{2T}} \quad (8)$$

where $\rho_o(\varepsilon)$ is the bare single-electron density of states and $A(\varepsilon, \omega) = -\frac{1}{\pi} \text{Im}(\omega + i0^+ - \varepsilon - \Sigma(\omega + i0^+))^{-1}$. In this adiabatic approximation, we calculate conductivity in the leading order of t^2 , in terms of quantities for $t = 0$ ($\rho(\varepsilon)$ and $A(\varepsilon, \omega)$).

These equations are easy to solve for arbitrary parameters of our model, but we illustrate our findings in Figure 3, by showing explicit results for half-filled cubic lattice with $\alpha = 0.3$. Our semiclassical solution is found to be valid in a broad pseudogap regime $T_c < T < T^*$, which spans almost an order of magnitude in temperature (for $E_F \ll 1$ we find $T_c \approx 0.03$ and $T^* \approx 0.25$). Here the conductivity displays unusual, insulating-like [$d\sigma(T)/dT > 0$], but rather weak (almost linear) temperature dependence [shown in Figure 3(b)], surprisingly similar to that observed in magnetite above the Verwey transition. Our microscopic theory confirms the heuristic picture first proposed in early work of Mott.⁹

VI. CONCLUSIONS

We argued that pseudogap behavior in Coulomb systems directly reflects strong frustration found in any system with very long-range repulsive interactions. We demonstrated that a quantitatively accurate strong-coupling description of this regime is possible using the interaction power α as a small parameter in the theory. The corresponding EDMFT equations were solved in the semiclassical regime where the pseudogap phenomena are most pronounced, explaining “bad-insulator” transport found in many puzzling experiments. It should be noted that, using appropriately formulated quantum impurity solvers,²¹ the same formulation could be extended to investigate low-temperature quantum critical behavior for the same class of models. This fascinating direction remains a challenge for future work.

VII. ACKNOWLEDGEMENT

The authors thank Seng Cheong, Misha Fogler, Daniel Khomskii, Andy Millis, Joerg Schmalian, Dan Tsui, and Kun Yang for useful discussions. This work was supported by the National High Magnetic Field Laboratory (YP, HT, SP, EM, and VD) and the NSF through Grants Nos. DMR-0542026 and DMR-1005751 (Y.P., H.T., and V.D.).

VIII. APPENDIX

A. Ewald Potential

In order to compute the effective potential of long-range interaction $1/|\vec{r}_{ij}|^\alpha$ in hypercubic lattice

$$V(\vec{r}_{ij}) = \sum_{n \in \mathbb{Z}} \frac{1}{|\vec{r}_{ij} + L\vec{n}|^\alpha}, \quad (9)$$

we use an Ewald-type summation²² with the help of the integral representation of^{23,24}

$$\frac{1}{|\vec{r}|^\alpha} = \frac{1}{\Gamma(\alpha/2)} \int_0^\varepsilon t^{\frac{\alpha}{2}-1} e^{-r^2 t} dt + \int_\varepsilon^\infty t^{\frac{\alpha}{2}-1} e^{-r^2 t} dt. \quad (10)$$

where $\Gamma(\alpha/2)$ is Gamma function. We switch the first term of the integral to a momentum sum because the sum does not converge rapidly in real space. Next, we use the representation²⁵

$$\begin{aligned} & \int d^d r \sum_{\vec{n}} \delta(\vec{r} - [L\vec{n} + \vec{r}_{ij}]) f(\vec{r}) \\ &= \int d^d r \sum_{\vec{G}_l} [e^{i\vec{G}_l \cdot \vec{r}} - \delta(\vec{r})] f(\vec{r}), \end{aligned} \quad (11)$$

where $f(\vec{r})$ is any arbitrary function and on the right-hand side the summation is over the vectors of the reciprocal lattice. We then integrate \vec{r} out and change the variable of the integration in the first term $t \rightarrow 1/t$. The final expression of the potential takes the form

$$\begin{aligned} V(\vec{r}) &= \frac{1}{\Gamma(\frac{\alpha}{2})} \sum_{\vec{n}} \varepsilon^\alpha \phi_{\frac{\alpha}{2}-1}(\varepsilon^2 |\vec{r} + \vec{n}L|^2) \\ &+ \frac{1}{\Gamma(\frac{\alpha}{2})\Omega} \sum_{\vec{k} \neq 0} \pi^{\frac{3}{2}} \varepsilon^{\alpha-3} \phi_{\frac{1-\alpha}{2}}\left(\frac{|\vec{k}|^2}{4\varepsilon^2}\right) e^{-i\vec{k} \cdot \vec{r}} \\ &- \frac{2\varepsilon^\alpha}{\Gamma(\frac{\alpha}{2})}, \end{aligned} \quad (12)$$

where in each component vector $k_i = 2\pi n_i$ and $n_i \in \mathbb{Z}$. At the maximum size of our Monte-Carlo simulation $L = 24$, the potential is accurate to the eighth decimal place with only $|n_i| = 3$ in each axis, and $\varepsilon = \sqrt{\pi}$.

B. Finite-size effects

In the vicinity of Wigner crystallization, the finite-size effects are very strong. The size dependence of the single particle density of states obtained from Monte-Carlo data for $d = 3$, $\alpha = 0.3$, and $T = 0.0554$ is shown in figure 4.

To carry out a careful finite-size scaling analysis of the DOS, we perform a two-Gaussian fit

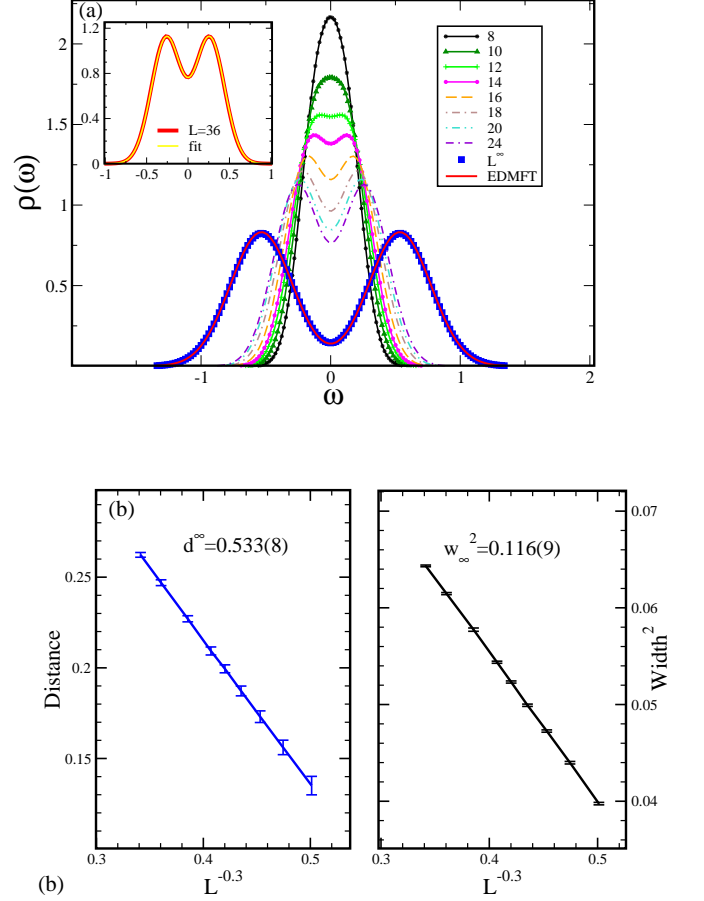


Figure 4: (Color online) (a) Two-Gaussian fit of the single particle density of states from different size of MC simulation. At this particular temperature, They fit perfectly with the EDMFT results. The fit form is shown in the inset. (b) The finite size scaling of the distance (left) and width-squared (right) of the two-Gaussian function for different sizes $L = 8, 10, 12, 16, 18, 20, 24$.

The nonlinear (two-Gaussian) fitting is done using IGOR 6.01. The fitting parameters, i.e., the distance between the Gaussian peaks and width squared as a function of $L^{-\alpha}$ is shown in the Fig 4(b). This allows us to perform an accurate extrapolation to $L = \infty$, and the result is found to be in excellent agreement with EDMFT prediction. Note how the finite-size result remains very far from the $L = \infty$ extrapolant even for our largest system size ($L = 24$). Accurate results, thus, simply cannot be obtained without such finite size scaling analysis.

-
- ¹ P. W. Anderson, Phys. Rev. **109**, 1492 (1958).
 - ² N. F. Mott, Proc. Phys. Soc. (London) **A62**, 416 (1949).
 - ³ E. Wigner, Phys. Rev. **46**, 1002 (1934).
 - ⁴ B. Tanatar and D. M. Ceperley, Phys. Rev. B **39**, 5005 (1989).
 - ⁵ J. Huang, D. S. Novikov, D. C. Tsui, L. N. Pfeiffer, and K. W. West, Physical Review B **74**, 201302 (2006).
 - ⁶ G. S. Boebinger, Y. Ando, A. Passner, T. Kimura, M. Okuya, J. Shimoyama, K. Kishio, K. Tamasaku, N. Ichikawa, and S. Uchida, Phys. Rev. Lett. **77**, 5417 (1996).
 - ⁷ C. Panagopoulos and V. Dobrosavljević, Phys. Rev. B **72**, 014536 (2005).
 - ⁸ E. Dagotto, Science **309**, 257 (2005).
 - ⁹ N. F. Mott, *Metal-Insulator Transition* (Taylor & Francis, London, 1990).
 - ¹⁰ B. Spivak, Phys. Rev. B **64**, 085317 (2001).
 - ¹¹ A. Kosevich, Sov. Phys. JETP **50**, 1218 (1979).
 - ¹² A. L. Efros, Phys. Rev. Lett. **68**, 2208 (1992).
 - ¹³ J. S. Thakur and D. Neilson, Phys. Rev. B **54**, 7674 (1996).
 - ¹⁴ A. P. Ramirez, Annu. Rev. Mater. Sci. **24**, 453 (1994).
 - ¹⁵ A. A. Pastor and V. Dobrosavljević, Phys. Rev. Lett. **83**, 4642 (1999).
 - ¹⁶ R. Chitra and G. Kotliar, Phys. Rev. Lett. **84**, 3678 (2000).
 - ¹⁷ S. Pankov and V. Dobrosavljević, Phys. Rev. Lett. **94**, 046402 (2005).
 - ¹⁸ J. Schmalian, D. Pines, and B. Stojković, Phys. Rev. B **60**, 667 (1999).
 - ¹⁹ M. P. Lilly, J. L. Reno, J. A. Simmons, I. B. Spielman, J. P. Eisenstein, L. N. Pfeiffer, K. W. West, E. H. Hwang, and S. DasSarma, Phys. Rev. Lett. **90**, 056806 (2003).
 - ²⁰ A. Georges, G. Kotliar, W. Krauth, and M. J. Rozenberg, Rev. Mod. Phys. **68**, 13 (1996).
 - ²¹ P. Werner, A. Comanac, L. deMedici, M. Troyer, and A. J. Millis, Phys. Rev. Lett. **97**, 076405 (2006).
 - ²² P. Ewald, Ann. Phys. **369**, 253 (1921).
 - ²³ U. Essmann, L. Perera, M. L. Berkowitz, T. Darden, H. Lee, H. G. Pedersen, J. Chem. Phys. **103**, 8577 (1995).
 - ²⁴ E. R. Smith, Proc. R. Soc. London **375**, 475 (1981).
 - ²⁵ M. Müller and S. Pankov, Phys. Rev. B **75**, 144201 (2007).
 - ²⁶ Strictly speaking, the nonlocal effects ignored by EDMFT are, for $\alpha \ll 1$, negligible throughout the broad pseudogap regime, but not in the narrow critical regime close to T_c .
 - ²⁷ The smallness of the melting temperature for a classical (continuum) Wigner crystal can similarly be understood⁴ by comparing it to the Debye temperature of sheer phonons.